induced relaxations of isolated rabbit aortic rings (Fig. 4). NO (10^{-8} to 10^{-5} M) caused transient, concentration-dependent relaxations (Fig. 4*a*). CTX (50 nM) alone did not significantly affect the maximal relaxation caused by each concentration of NO (Fig. 4*a*, *b*), but did change the time course of relaxation (Fig. 4*a*), and significantly reduced the integrated relaxation (Fig. 4*c*). Inhibition of guanylate cyclase by methylene blue (10^{-4} M) caused a significant reduction in cGMP content of arterial rings stimulated with NO (Fig. 4*f*). However, significant relaxations of the rings to NO (10^{-7}–10^{-5} M) persisted and became less transient in the presence of methylene blue (Fig. 4*d*). These methylene blue-resistant, NO-induced relaxations were significantly blocked by CTX (Fig. 4*d*, *e*). Thus, inhibiting guanylate cyclase with methylene blue unmasked cGMP-independent relaxations to NO which are probably mediated by the direct effect of NO on K^+_{Ca} channels in the intact rabbit aorta.

In summary, this study demonstrates that both exogenous NO and native EDRF can directly activate K^+_{Ca} channels, which could cause hyperpolarization and relaxation of vascular smooth muscle[15–17] independently of cGMP. It was shown recently that ACh does not increase cGMP in atherosclerotic rabbit carotid arteries, but nevertheless causes normal relaxations which are inhibited similarly by CTX and an NO-synthase blocker[18]. Together with our present findings, these studies suggest that the NO-mediated cGMP-independent activation of K^+_{Ca} channels may circumvent the lack of the cGMP-dependent pathway to relax atherosclerotic arteries. □

Received 6 October 1993; accepted 1 March 1994.

1. Palmer, R. M. J., Ferrige, A. G. & Moncada, S. *Nature* **327,** 524–526 (1987).
2. Stamler, J. S., Singel, D. J. & Loscalzo, J. *Science* **258,** 1898–1902 (1992).
3. Knowles, R. G. & Moncada, S. *Trends biochem. Sci.* **17,** 399–402 (1992).
4. Lincoln, T. M. & Cornwell, T. L. *Blood Vessels* **28,** 129–137 (1991).
5. Lincoln, T. M. & Cornwell, T. L. *FASEB J.* **7,** 328–338 (1993).
6. Robertson, B. E., Schubert, R., Hescheler, J. & Nelson, M. T. *Am. J. Physiol.* **265,** C299–C303 (1993).
7. Taniguchi, J., Furukawa, K.-I. & Shigekawa, M. *Pflügers Arch.* **423,** 167–172 (1993).
8. Malinski, T. *et al. Biochem. biophys. Res. Commun.* **193,** 1076–1082 (1993).
9. White, R. E. *et al. Nature* **361,** 263–266 (1993).
10. Moncada, S., Radomski, M. W. & Palmer, R. M. J. *Biochem. Pharmac.* **37,** 2495–2501 (1988).
11. Griffith, T. M., Edwards, D. H., Lewis, M. J., Newby, A. C. & Henderson, A. H. *Nature* **308,** 645–647 (1984).
12. Stamler, J. S. *et al. Proc. Natn. Acad. Sci. U.S.A.* **89,** 444–448 (1992).
13. Lei, S. Z. *et al. Neuron* **8,** 1087–1099 (1992).
14. Lipton, S. A. *et al. Nature* **364,** 626–632 (1993).
15. Tare, M., Parkington, H. C., Coleman, H. A., Neild, T. O. & Dusting, G. J. *Nature* **346,** 69–71 (1990).
16. Krippeit-Drews, P., Morel, N. & Godfraind, T. *J. Cardiovasc. Pharmac.* **20,** S72–S75 (1992).
17. Brayden, J. E. & Nelson, M. T. *Science* **256,** 532–535 (1992).
18. Najibi, S., Cowan, C. L., Palacino, J. J. & Cohen, R. A. *Am. J. Physiol.* **266** (Heart Circ. Physiol. 35) (1994).
19. Taha, Z., Kiechle, F. & Malinski, T. *Biochem. Biophys. Res. Commun.* **188,** 734–739 (1992).
20. Hamill, O. P., Marty, A. Neher, E., Sakmann, B. & Sigworth, F. *Pflügers Arch.* **391,** 85–100 (1981).
21. Barrett, J. N., Magleby, K. L. & Pallotta, B. S. *J. Physiol.* **331,** 211–230 (1982).
22. Benham, C. D., Bolton, T. B., Lang, R. J. & Takewaki, T. *J. Physiol.* **371,** 45–67 (1986).
23. Singer, J. J. & Walsh, J. V. *Pflügers Arch.* **408,** 98–11 (1990).
24. Bolotina, V., Omelyanenko, V., Heyes, B., Ryan, U., Bregestovski, P. *Pflügers Arch.* **415,** 262–268 (1989).
25. Toro, L. & Stefani, E. *J. Bioenerg. Biomembr.* **23,** 561–576 (1991).
26. Miller, C., Moczydlowski, E., Latorre, R. & Phillips, M. *Nature* **313,** 316–318 (1985).
27. Cowan, C. L., Palacino, J. J., Najibi, S. & Cohen, R. A. *J. pharmac. exp. Ther.* **266,** 1482–1488 (1993).
28. Wolin, M. S., Cherry, P. D., Rodenburg, J. M., Messina, E. J. & Kaley, G. *J. pharmac. Exp. Ther.* **254,** 872–876 (1990).

ACKNOWLEDGEMENTS. We thank A. Cayatte and R. Weisbrod for help with SMC culture, D. Tillotson and K. Bokvist for technical support in designing the patch-clamp setup, S. Levy for determination of free Ca^{2+} in the solutions and B. Bean for reviewing the manuscript and for helpful comments. The studies were supported by the NIH.

Anchoring of protein kinase A is required for modulation of AMPA/kainate receptors on hippocampal neurons

Christian Rosenmund*, Daniel W. Carr, Susan E. Bergeson, Gajanan Nilaver†, John D. Scott & Gary L. Westbrook‡

Vollum Institute, and † Department of Neurology, Oregon Health Sciences University, Portland, Oregon 97201, USA

PHOSPHORYLATION of molecules involved in synaptic transmission by multifunctional protein kinases modulates both pre- and postsynaptic events in the central nervous system[1,2]. The positioning of kinases near their substrates may be an important part of the regulatory mechanism. The A-kinase-anchoring proteins (AKAPs; ref. 3) are known to bind the regulatory subunit of cyclic AMP-dependent protein kinase A with nanomolar affinity[4–6]. Here we show that anchoring of protein kinase A by AKAPs is required for the modulation of α-amino-3-hydroxy-5-methyl-4-isoxazole-propionic acid (AMPA)/kainate channels[4,5]. Intracellular perfusion of cultured hippocampal neurons with peptides derived from the conserved kinase binding region of AKAPs prevented the protein kinase A-mediated regulation of AMPA/kainate currents as well as fast excitatory synaptic currents. This effect could be overcome by adding the purified catalytic subunit of protein kinase. A control peptide lacking kinase-binding activity had no effect. To our knowledge, these results provide the first evidence that anchoring of protein kinase A is crucial in the regulation of synaptic function.

* Present address: The Salk Institute, 10010 North Torrey Pines Road, La Jolla, California 92037, USA.
‡ To whom correspondence should be addressed.

Cyclic AMP and its principal target, cAMP-dependent protein kinase, regulate the release of transmitter as well as postsynaptic receptors and channels[1–3,7–9]. Although multiple effectors can elevate cAMP, a limited set of substrates are phosphorylated in response to activation by particular hormones or neurotransmitters. Several mechanisms have been proposed to account for this specificity[10–15].

Biochemical and immunocytochemical analysis demonstrated that several AKAPs were present in cultured hippocampal neurons and were colocalized with the regulatory subunit RII of protein kinase A (PKA) in the soma and dendrites (Fig. 1*A*). The hippocampal neurons were immunoreactive when stained with antibodies prepared against RII (Fig. 1*A*, *a* and *b*) or AKAP79 (Fig. 1*A*, *c* and *d*), the human homologue of AKAP150 (ref. 3). Multiple RII-binding proteins with relative molecular masses of 50–200K were detected by the solid-phase binding of RII to AKAPs (Fig. 1*B*, lane 1). However, RII binding was blocked by preincubation with a 24-amino-acid peptide (Ht31 peptide[6]) derived from a conserved amphipathic helix common to the family of AKAP proteins (Fig. 1*B*, lane 2). The remaining 50K band was RII itself, as determined by western blots (Fig. 1*B*, lane 4). A 16-amino-acid control peptide derived from Ht31 peptide did not block binding of RII to AKAPs (Fig. 1*B*, lane 3). These peptides provide the reagents needed to test the functional consequences of A-kinase-anchoring in neurons.

PKA-dependent phosphorylation is required to maintain the function of AMPA/kainate channels in hippocampal neurons[7,8]. In the absence of ATP, whole-cell currents evoked by kainate (20 μM) gradually declined over 25 min to 50.9 ± 5.2% ($n = 8$) (Fig. 2*b*). This 'rundown' was prevented by addition of ATP (87.4 ± 3.2, $n = 12$, $P < 0.001$). The current also gradually decreased in the presence of ATP and the peptide PKI(5–24), a potent and specific inhibitor of the catalytic subunit of PKA (61.8 ± 4.1%, $n = 11$, $P < 0.001$) (Fig. 2*a*, *b*). This confirmed that endogenous PKA modulates channel activity. To test the role of AKAPs in localizing PKA near the channel, anchoring inhibitor peptides were added to the whole-cell pipette. As shown in Fig.

© 1994 Nature Publishing Group

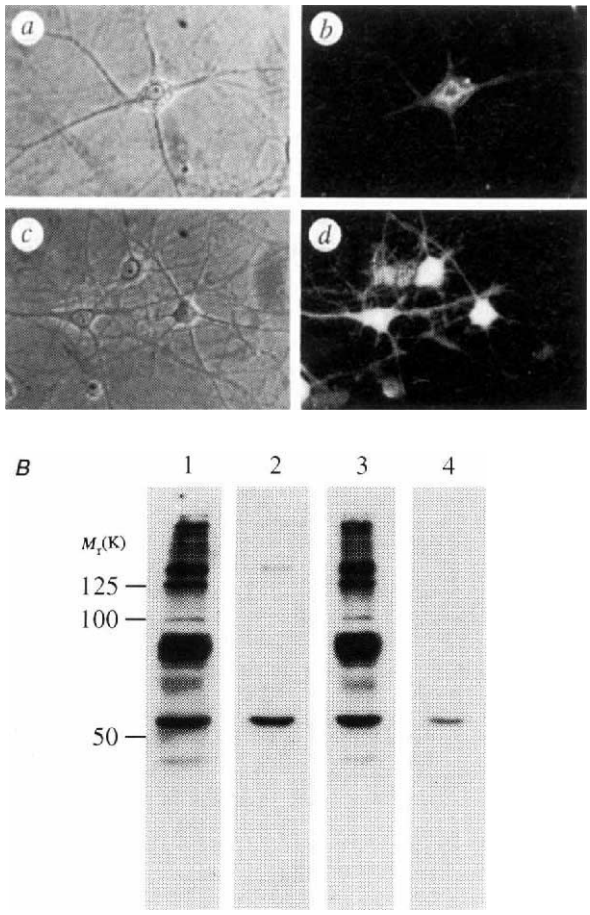

FIG. 1 Expression of AKAPs in cultured hippocampal neurons. *A*, RII and AKAP 150 co-exist in the same cellular compartments of cultured hippocampal neurons. *a*, Phase contrast photomicrograph of a cultured hippocampal neuron; *b*, indirect immunofluorescence of the same cell incubated with affinity-purified RII antiserum (1:1,000 dilution). RII is excluded from the nucleus and is distributed in both the soma and neurites. *c* and *d*, Phase contrast photomicrograph and indirect immunofluorescence of neurons incubated with 1:1,000 AKAP 79 antiserum, the human homologue of murine AKAP 150 that is concentrated in postsynaptic densities[3]. Specificity of immunostaining with RII and AKAP150 antibodies was confirmed by the absence of fluorescence in parallel cultures incubated with nonimmune sera, and with the sera solid phase absorbed with homologous but not heterologous antigens (data not shown). Prominent staining of the soma and neurites suggests that RII and AKAP 150 are present in the same cellular compartments. *B*, Anchoring inhibitor peptides block the solid-phase binding of RII to AKAPs. Lane 1 shows the pattern of AKAPs expressed in cultured hippocampal neurons, where several prominent RII-binding bands ranging in size from 50K to 200K were detected. All RII-AKAP interactions were blocked when filters were incubated in the presence of 0.4 μM Ht31 peptide (residues 494–515; lane 2), consistent with our previous observations[6]. In contrast, incubation of filters in the presence of a Ht31 control peptide (residues 494–509; lane 3) did not block the solid-phase binding of RII to AKAPs. The presence of RII in cultured hippocampal neurons was confirmed by western blot using affinity-purified antiserum (lane 4).

METHODS. Primary dissociated hippocampal cultures were prepared as described[28]. Hippocampal neurons, grown on coverslips for 7 days, were fixed with ice-cold methanol. Slides were washed for 1 h at room temperature in Tris-buffered saline/BSA/Brij 56 solution, then incubated overnight at 4 °C with primary antibodies. Immune complexes were tagged by incubation with FITC-conjugated goat anti-rabbit secondary antibodies (1:100 dilution) for 2 h at room temperature. Detection of fluorescence was by excitation at 470 nm on a Leitz fluorescent microscope. The presence of AKAPs and RII was investigated by the RII-overlay procedure for anchoring proteins[6]. Protein samples (50 μg) were separated on a 10% SDS-polyacrylamide gel. Blots were incubated in a blotto solution (Tris-buffered saline (pH 7.4)/5% w/v dry milk/0.1% w/v BSA) containing purified murine RIIa (200 ng ml^{-1}) and solid-phase RII was detected by western blotting with affinity-purified RII antibodies (1:2,000) using an ECL detection kit (Amersham).

2, the anchoring inhibitor peptide derived from Ht31 (1 μM) inhibited AMPA/kainate currents to the same extent as PKI (64.9 ± 3.2%, $n = 11$, $P < 0.0001$). The effects of Ht31 peptide and PKI were not additive (Fig. 2*c*). These results indicate that PKA localization is required for the modulation of AMPA/kainate currents.

We considered that Ht31 peptide might compete with AKAPs, leading to a gradual displacement of type II PKA holoenzyme from the anchoring sites. Consistent with this, there was an initial delay in the action of the Ht31 peptide. Similar inhibition of AMPA/kainate currents was observed with a peptide derived from the RII binding region of AKAP79 (1 μM, 68.3 ± 3.3%, $n = 12$, $P < 0.001$). In addition, a 16-amino-acid control peptide that does not bind RII (Fig. 1) had no effect on kainate currents (85 ± 4.1%, $n = 7$), indicating that the action of the anchoring inhibitor peptides was specific. The action of Ht31 peptide could be overcome by the catalytic subunit (0.3 μM), suggesting that the anchoring inhibitor peptides interfered with PKA-dependent phosphorylation, but did not directly inhibit the kinase or channel gating. Currents evoked by AMPA (1 μM, $n = 6$) also ran down in the absence of ATP, and Ht31 peptide reduced the current ($n = 6$), suggesting that the modulated channels were low-affinity AMPA receptors[16]. As low-affinity AMPA receptors are presumed to be heteromers of GluR1–4 which lack consensus PKA sites[17,21], phosphorylation probably occurs at a 'non-consensus' site[22] or involves a regulatory protein near the channel.

Simulation of PKA by forskolin also enhances the synaptic currents mediated by AMPA/kainate receptors in hippocampal neurons[8,23]. To determine the effect of Ht31 peptide on spontaneous excitatory postsynaptic currents (e.p.s.cs) mediated by AMPA/kainate receptors, spontaneous e.p.s.cs were analysed at the beginning of whole-cell recording and after 25 min of intracellular dialysis. In the presence of ATP, the amplitude of spontaneous e.p.s.cs was well maintained (90.4 ± 4.7%; $n = 7$), with no change in spontaneous e.p.s.cs frequency or duration. Ht31 peptide caused a significant decrease in spontaneous e.p.s.cs amplitude (73.9 ± 3.7%; $n = 6$, $P < 0.02$) with no change in the decay of the current (Fig. 3*a*, *b*). As expected, there was no change in e.p.s.cs frequency, suggesting that Ht31 peptide in the postsynaptic cell did not affect release from the presynaptic terminal. As previously described[8,23], forskolin (50 μM, $n = 5$) enhanced the spontaneous e.p.s.c. frequency (222 ± 48%), presumably by a presynaptic mechanism, but produced only a small increase in amplitude (105 ± 48%), indicating that endogenous activity of PKA was sufficient to maintain the synaptic AMPA/kainate channels. Thus AKAP–PKA interactions are also important in the regulation of synaptically activated AMPA/kainate channels.

These results offer physiological evidence that anchoring of kinases by AKAPs are critical in the phosphorylation of target proteins. AKAPs appear to be bifunctional molecules that have a conserved kinase-binding site, but unique targeting domains responsible for localizing AKAP–PKA complexes to cellular compartments[3,5,24,26]. The anchoring inhibitor peptides disrupted all PKA–AKAP interactions, thus the specific AKAP responsible for the regulation of AMPA/kainate channel activity remains to be determined. AKAP150 is one candidate as it is present in rat and mouse postsynaptic densities[3]. These results suggest that the local concentration of kinase is likely to be important in regulating PKA-dependent phosphorylation at the

© 1994 Nature Publishing Group

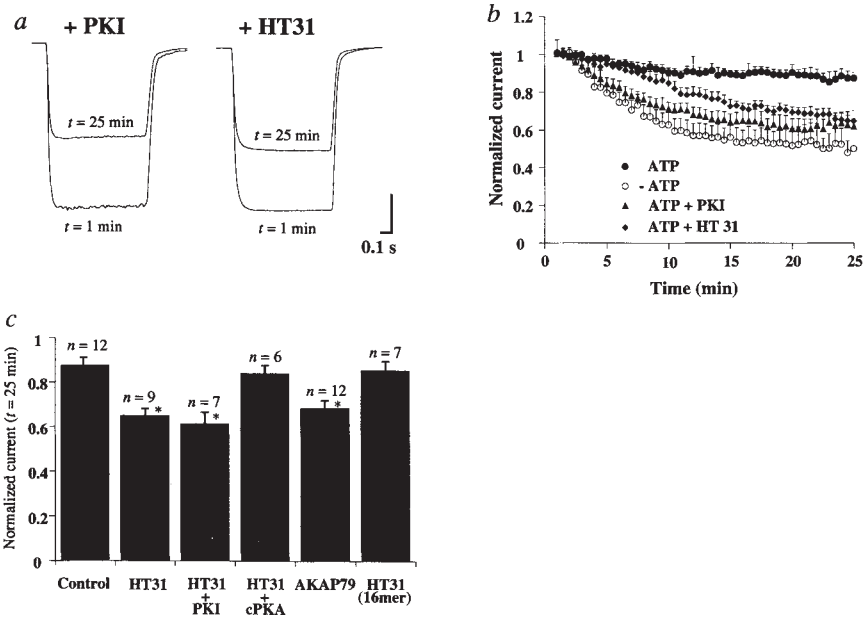

FIG. 2 Displacement of RII subunit by anchoring inhibitor peptides blocks the regulation AMPA/kainate channels by PKA. *a*, Inward currents evoked by kainate (20 μM) at 1 and 25 min after the start of whole-cell recordings are superimposed. Left, the current gradually decreased in presence of PKI(5–24) peptide (1 μM) in the recording pipette. Right, a similar decrease in channel activity was seen during whole-cell dialysis with Ht31 peptide (1 μM), a synthetic 24-amino-acid peptide derived from A-kinase-anchoring protein Ht31, which is a competitive inhibitor of RII anchoring. The holding potential was −60 mV. ATP (5 mM) was included in the patch pipette. Calibration bar is 200 pA (left panel) and 360 pA (right panel). *b*, The time course of AMPA/kainate currents during whole-cell recording. Responses were normalized to the peak amplitude at 1 min after the start of recording. Symbols indicate mean ±s.e. The loss of activity was similar in the absence of ATP (rundown) or when PKI or Ht31 peptide was added. The onset of action of Ht31 peptide was slightly delayed (see text). *c*, Amplitude of AMPA/kainate currents after 25 min of recording in the presence of 5 mM ATP in the patch pipette. The control and Ht31 peptide results are taken from *b*. Additional histogram bars show mean current amplitudes with the following reagents in the patch pipette: Ht31 peptide (1 μM) and PKI (1 μM); Ht31 peptide and catalytic subunit (cPKA, 0.3 μM); AKAP 79 anchoring-inhibitory peptide (1 μM); and a control peptide derived from Ht31 peptide that does not bind RII (Ht31, 16-mer). Asterisks indicate statistical significance reduction in current compared to control.

METHODS. Whole-cell recordings of neurons 5–12 days in culture were made with an Axopatch 1C amplifier (Axon Instruments). The intracellular medium under recording conditions contained: 165 mM NaCl, 2.4 mM KCl, 2 mM $CaCl_2$, 1 mM $MgCl_2$, 10 mM glucose, 10 mM HEPES, 1 μM tetrodotoxin (TTX), 100 μM picrotoxin, pH 7.2; 325 mOsm. Recording pipettes had a resistance of 1–2 MΩ and contained 155 mM caesium gluconate, 10 mM HEPES, 10 mM BAPTA, 5 mM Mg-ATP, 2 mM $MgCl_2$, pH 7.3; 315 mOsm. Only neurons with series resistance of <8 MΩ were included in the analysis. Series resistance (70–90%) and the cell capacitance were compensated and continuously monitored during recording. Reagents were introduced into the cell by diffusion from the pipette; exchange times for small peptides was estimated to be 1–3 min based on test reagents[29]. AMPA/kainate channel activity was measured by applying agonist pulses at set intervals (0.3–1s; every 30 s). Solutions were exchanged using a series of flow pipes (400 μM internal diameter) positioned within 100–200 μm of the neuron, and connected to gravity-fed reservoirs. Each flow pipe was controlled by solenoid valve and the assembly was moved with a piezoelectric bimorph (Vernitron, USA). Membrane currents were sampled at 1–2 kHz, filtered at 500 Hz and stored on an IBM-compatible computer using PClamp (V.5.5, Axon Instruments). For statistical analysis, the agonist-evoked membrane current at 1 min was compared with the response after 25 min of recording. Data are expressed as per cent of control ±s.e. Significance was tested using analysis of variance with the Bonferroni–Dunn test for multiple comparisons; *P* values are given when significant.

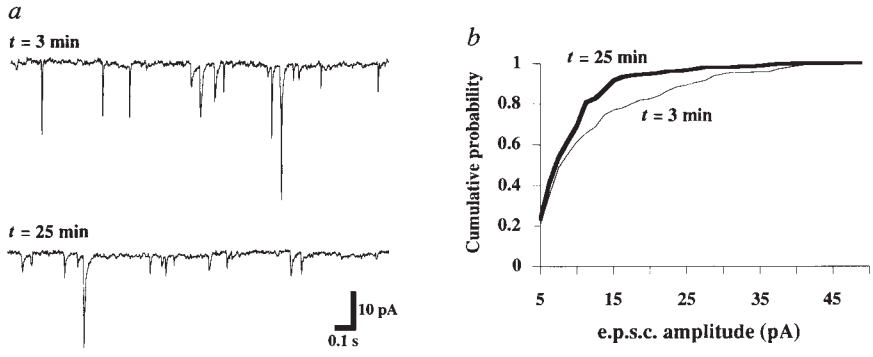

FIG. 3 Dialysis with Ht31 peptide reduced the amplitude of spontaneous e.p.s.cs. *a*, Spontaneous AMPA/kainate-receptor-mediated e.p.s.cs at the beginning (3 min) and end (25 min) of the recording period at a holding potential of −60 mV. *b*, Cumulative probability histogram of spontaneous e.p.s.c. amplitudes from the same neuron as in *a*. The amplitudes of spontaneous e.p.s.cs were reduced by Ht31 peptide (1 μM). The threshold for peak detection of spontaneous e.p.s.cs for this neuron was set at 4 pA and data were binned at 2 pA intervals. The frequency of spontaneous e.p.s.cs did not change in the presence of Ht31 peptide. The mean frequency was 21 Hz at 3 min and 22 Hz at $t = 25$ min.

METHODS. The extracellular solution contained TTX (1 μM), 5 mM Mg^{2+} with no added glycine, picrotoxin (100 μM) and strychnine (2 μM) to block sodium channels, NMDA receptors and GABA/glycine channels, respectively. The peak amplitude and the half-width (duration at 50% of peak amplitude) for each spontaneous e.p.s.c. was measured using AXOGRAPH software (Axon Instruments). Threshold for peak detection was set for each cell depending on the baseline noise and held constant throughout the recording period. Currents were acquired in 1-min epochs, filtered at 1-2 kHz (8-pole Bessel) and sampled at 2–4 kHz. Significance was tested using Student's *t*-test.

synapse. Given the presence of multiple phosphoproteins in the postsynaptic density and the existence of targeting proteins for other kinases[27], compartmentalization of kinases may be a general mechanism for regulating the phosphorylation state of synaptic proteins, including receptors, enzymes and cytoskeletal elements. □

Received 9 November 1993; accepted 21 February 1994.

1. Greengard, P., Valtorta, F., Czernik, A. J. & Benfenati, F. *Science* **259,** 780–784 (1993).
2. Levitan, I. A. *Rev. Neurosci.* **11,** 119–136 (1988).
3. Carr, D. W., Stofko-Hahn, R. E., Fraser, I. D. C., Cone, R. D. & Scott, J. D. *J. biol. Chem.* **267,** 16816–16823 (1992).
4. Bregman, D. B., Bhattacharyya, N. & Rubin, C. S. *J. biol. Chem.* **264,** 4648–4656 (1989).

© 1994 Nature Publishing Group

5. Carr, D. W. *et al. J. biol. Chem.* **266,** 14188–14192 (1991).
6. Carr, D. W., Hausken, Z. E., Fraser, I. D. C., Stofko-Hahn, R. E. & Scott, J. D. *J. biol. Chem.* **267,** 13376–13382 (1992).
7. Wang, L.-Y., Salter, M. W. & MacDonald, J. F. *Science* **253,** 1132–1135 (1991).
8. Greengard, P., Jen, J., Nairn, A. C. & Stevens, C. F. *Science* **253,** 1135–1138 (1991).
9. Swope, S., Moss, S. J., Blackstone, C. D. & Huganir, R. L. *FASEB* **6,** 2514–2523 (1992).
10. Uhler, M. D., Chrivia, J. C. & McKnight, G. S. *J. biol. Chem.* **261,** 15360–15363 (1986).
11. Hofmann, F., Beavo, J. A., Bechtel, P. J. & Krebs, E. G. *J. biol. Chem.* **250,** 7795–7801 (1975).
12. Barsony, J. & Marks, S. J. *Proc. natn. Acad. Sci. U.S.A.* **87,** 1188–1192 (1990).
13. Bacskai, B. J. *et al. Science* **260,** 222–226 (1993).
14. Rubin, C. S., Rangel-Aldao, R., Sarkar, D., Ehrlichman, J. & Fleischer, N. *J. biol. Chem.* **254,** 3797–3805 (1979).
15. Corbin, J. D., Keely, S. L. & Park, C. R. *J. biol. Chem.* **250,** 218–225 (1975).
16. Patneau, D. K. & Mayer, M. L. *J. Neurosci.* **10,** 2385–2399 (1990).
17. Gasic, G. P. & Hollmann, M. *A. Rev Physiol.* **54,** 507–536 (1992).
18. Sommer, B. & Seeburg, P. *Trends pharmac. Sci.* **13,** 291–296 (1992).
19. Egebjerg, J., Bettler, B., Hermans-Borgmeyer, I. & Heinemann, S. *Nature* **351,** 745–748 (1991).
20. Wang, L.-Y., Taverna, F. A., Huang, X.-P., MacDonald, J. F. & Hampson, D. R. *Science* **259,** 1173–1175 (1993).
21. Raymond, L. A., Blackstone, C. D. & Huganir, R. L. *Nature* **361,** 637–641 (1993).
22. Keller, B. U., Hollmann, M., Heinemann, S. & Konnerth, A. *EMBO. J.* **11,** 891–896 (1992).
23. Chavez-Noriega, L. E. & Stevens, C. F. *Brain Res.* **574,** 85–92 (1992).
24. Threurfauf, W. & Vallee, R. *J. biol. Chem.* **257,** 3284–3290 (1982).
25. De Camilli, P., Moretti, M., Donini, S. D., Walter, U. & Lohmann, S. M. *J. Cell Biol.* **103,** 189–203 (1986).
26. Glantz, S. B., Amat, J. A. & Rubin, C. S. *Molec. Biol. Cell* **3,** 1215–1228 (1992).
27. Hubbard, M. J. & Cohen, P. *Trends biochem. Sci.* **18,** 172–177 (1993).
28. Legendre, P. & Westbrook, G. L. *J. Physiol., Lond.* **429,** 429–449 (1990).
29. Rosenmund, C. & Westbrook, G. L. *J. Physiol., Lond.* **470,** 705–729 (1993).

ACKNOWLEDGEMENTS. This work was supported by grants from the USPHS (G.L.W., J.D.S. and D.W.C.). We thank J. Volk for the preparation of the cell cultures.

Antigen-specific human antibodies from mice comprising four distinct genetic modifications

Nils Lonberg, Lisa D. Taylor, Fiona A. Harding, Mary Trounstine, Kay M. Higgins, Stephen R. Schramm, Chiung-Chi Kuo, Roshanak Mashayekh, Kathryn Wymore, James G. McCabe, Donna Munoz-O'Regan, Susan L. O'Donnell, Elizabeth S. G. Lapachet, Tasha Bengoechea, Dianne M. Fishwild, Condie E. Carmack, Robert M. Kay* & Dennis Huszar

GenPharm International, 297 North Bernardo Avenue, Mountain View, California 94043, USA

HUMAN sequence monoclonal antibodies, which in theory combine high specificity with low immunogenicity, represent a class of potential therapeutic agents. But nearly 20 years after Köhler and Milstein first developed methods for obtaining mouse antibodies[1], no comparable technology exists for reliably obtaining high-affinity human antibodies directed against selected targets. Thus, rodent antibodies[2], and *in vitro* modified derivatives of rodent antibodies[3–5], are still being used and tested in the clinic. The rodent system has certain clear advantages; mice are easy to immunize, are not tolerant to most human antigens, and their B cells form stable hybridoma cell lines. To exploit these advantages, we have developed transgenic mice that express human IgM, IgG and Igκ in the absence of mouse IgM or Igκ. We report here that these mice contain human sequence transgenes that undergo *V(D)J* joining, heavy-chain class switching, and somatic mutation to generate a repertoire of human sequence immunoglobulins. They are also homozygous for targeted mutations that disrupt *V(D)J* rearrangement at the endogenous heavy- and κ light-chain loci. We have immunized the mice with human proteins and isolated hybridomas secreting human IgGκ antigen-specific antibodies.

* To whom correspondence should be addressed.

FIG. 1 Human immunoglobulin heavy- and light-chain minilocus transgenes rescue the B-cell compartment of Ig$^-$ mutant mice. *a*, The KCo4 and HC2 transgene inserts are depicted before microinjection. The HC2 transgene is described elsewhere[13]. The light-chain minilocus, KCo4, is created by co-injection of two overlapping DNA fragments, each of which is propagated within a different plasmid. *b*, Flow cytometric analysis of fluorescent-stained cells isolated from spleens of 4 mice with different genotypes. For each of the 2-colour panels, the relative number of cells in each of the displayed quadrants is given as per cent of a 3-parameter, live-lymphocyte, gate based on propidium iodide staining and light scatter. The fraction of B220$^+$ cells in each of the samples displayed in the bottom row is given as a per cent of the lymphocyte light-scatter gate. Left column: control mouse (no. 9944, 6-week-old female J$_H^{+/-}$, J$\kappa^{+/-}$). Second column: human heavy-chain transgenic (no. 9877, 6-week-old female J$_H^{-/-}$, J$\kappa^{-/-}$, HC2 line 2550$^+$). Third column: human κ light-chain transgenic (no. 9878, 6-week-old female J$_H^{-/-}$, J$\kappa^{-/-}$, KCo4 line 4437$^+$). Right column: double transgenic (no. 9879, 6-week-old female J$_H^{-/-}$, J$\kappa^{-/-}$, HC2 line 2550$^+$, KCo4 line 4437$^+$). Top row: expression of mouse λ light chain (*x*-axis) and human κ light chain (*y*-axis). Second row: expression of human μ heavy chain (*x*-axis) and human κ light chain (*y*-axis). Third row: expression of mouse μ heavy chain (*x*-axis) and mouse κ light chain (*y*-axis). Bottom row: expression of mouse B220 antigen (log fluorescence: *x*-axis; cell number: *y*-axis). *c*, Comparison of pre-B- and B-cell numbers in wild-type (●) and double-transgenic/double-deletion (○) mice. Bone marrow, spleen and peritoneal cells isolated from three 3-month-old female double-transgenic/double-deletion (J$_H^{-/-}$, J$\kappa^{-/-}$, HC2 line 2550$^+$, KCo4 line 4437$^+$) and 3 age-matched female wild-type B6CBF1 mice. The fraction of pre-B cells (B220$^+$/IgM$^-$) and B cells (B220$^+$/IgM$^+$) for each sample was determined on a wide scatter (including large and small lymphocytes, neutrophils and macrophages), propidium-iodide-negative gate. *d*, Secreted immunoglobulin levels in the serum of double-transgenic/double-deletion mice. Human μ, γ and κ, and mouse γ and λ from 18 individual HC2/KCo4 double-transgenic mice homozygous for endogenous heavy and κ-light chain locus disruptions. Mice (+) HC2 line 2550 (~5 copies of HC2 per integration), KCo4 line 4436 (1–2 copies of KCo4 per integration); (○) HC2 line 2550, KCo4 line 4437 (~10 copies of KCo4 per integration); (×) HC2 line 2550, KCo4 line 4583 (~5 copies of KCo4 per integration); (□) HC2 line 2572 (30–50 copies of HC2 per integration), KCo4 line 4437; (△) HC2 line 5467 (20–30 copies of HC2 per integration), KCo4 line 4437.

METHODS. Construction of the light chain minilocus (KCo4): a Vκ specific oligonucleotide was used to probe a human placental genomic DNA phage library (Clonetech). DNA fragments containing Vκ segments from positive phage clones were subcloned into plasmid vectors. Four different clones (vκ65.3, vκ65.5, vκ65.8 and vκ65.15) with open reading frames, intact splice acceptor and donor sequences, and intact recombination sequences were cloned together in a single plasmid, pKV4, with a 21-kb insert. The 3′ V segment in this plasmid, vκ65.3, was also subcloned into a second plasmid together with a 22-kb κ constant region fragment that covers the κ constant region from 4.5 kb upstream of Jκ1 to 13 kb downstream of Cκ. Transgenic mice: DNA fragments were isolated from plasmid vector DNA[17] by agarose gel electrophoresis and microinjected into the pronuclei of half-day (C57BL/6J × CBA/J)F$_2$ embryos[18]. Twenty-three light-chain-positive and 18 ►

We constructed minilocus transgenes by stitching together non-contiguous genomic fragments containing functional coding and non-coding units of the human heavy- and κ light-chain immunoglobulin loci (Fig. 1*a*). The heavy-chain transgene, HC2, consists of an 80-kilobase (kb) DNA fragment containing four functional V segments, 15 D segments, 6 J segments, the μ and γ1 coding exons together with their respective switch regions, as well as the Jμ intronic enhancer and the rat 3′ heavy-chain enhancer[6]. All of the sequences are human except for the non-coding 3′ enhancer.

The light-chain transgene, KCo4, is derived from the co-integration of two individually cloned DNA fragments at a single site in the mouse genome. The fragments together comprise four functional Vκ segments, 5 J segments, the Cκ exon, and both the intronic and downstream enhancer elements[7,8]. All of the sequences are of human origin. Because the two fragments share

© 1994 Nature Publishing Group